Meteorol Atmos Phys
DOI 10.1007/s00703-010-0109-5

ORIGINAL PAPER

Observational analysis of moisture evolution and variability in the boundary layer during the dryline on 22 May 2002

M. H. Weldegaber · B. B. Demoz · L. C. Sparling · R. Hoff · S. Chiao

Received: 19 March 2010 / Accepted: 16 November 2010

Abstract An observational analysis of boundary layer moisture evolution during the dryline on 22 May 2002 is presented. This dryline occurred during the International H_2O Project (IHOP) and was well observed by a variety of instruments at the intensive observing region (IOR), Homestead site. Although the observed strong upward air motion and the well-mixed boundary layer favored convection, the dryline did not trigger a convective storm. Several operational and research forecast models predicted deep convection at the IOR. High spatial and temporal resolution observational data from National Aeronautics and Space Administration (NASA) lidar instruments, Atmospheric Emitted Radiance Interferometer (AERI), sounding profiles and simulation results are used to investigate the role of moisture during this dryline. It is hypothesized that in addition to convection and lifting, abundant, deep and persistent moisture is required for a dryline to trigger convection. The possible reason why the dryline failed to trigger convection over the IOR is discussed.

M. H. Weldegaber (✉) · L. C. Sparling · R. Hoff
University of Maryland, Baltimore County (UMBC), Baltimore, MD 21250, USA
e-mail: mengs1@umbc.edu

M. H. Weldegaber · L. C. Sparling · R. Hoff
Joint Center for Earth Systems Technology, Baltimore, MD 21228, USA

B. B. Demoz
Department of Physics and Astronomy, Howard University, Washington, DC 20059, USA

S. Chiao
Marine and Environmental Systems Florida Institute of Technology, Melbourne, FL 32901, USA

1 Introduction

The U.S. Southern Great Plains (SGP) is a favored region for severe storms and flash floods. In particular, frequent storms in the late spring and summer occur near the Oklahoma–Texas border, a region where the dryline is frequently observed. The dryline over the SGP is a mesoscale boundary separating warm, moist maritime air from the Gulf of Mexico and hot, dry continental air from the arid elevated terrain of the southwestern U.S. and northern Mexico (Schaefer 1986). Convection along a dryline is associated with mesoscale low-level convergence and lifting of moist air that often triggers severe thunderstorms. In contrast to frontal boundaries that have strong dynamic consistency both in time and in space, the dynamics that control dryline structure and evolution can vary markedly over very short temporal and spatial scales. For this reason, the accompanying severe weather has been a forecasting challenge.

Since the dryline is primarily a boundary layer phenomenon, understanding the evolution of moisture, temperature, and the general characteristics of the boundary layer during dryline conditions is a critical component of severe-weather forecasting in the SGP. The concept of the "dry front" by Fujita (1958) and "instability line" by Beebe (1958) and their role in thunderstorms were identified in the late 1950s. Since then many dryline studies have been conducted (e.g., Staff Members 1963; Schaefer 1973; Parsons et al. 1991; Sun and Wu 1992; Bluestein and Parker 1993; Hane et al. 1993; Ziegler et al. 1997; Shaw et al. 1997; Crawford and Bluestein 1997; Atkins et al. 1998; Wilson and Schreiber 1986, etc.). Among the most intriguing mesoscale phenomena in the SGP is the role of the dryline in convection initiation. Convection initiation along a dryline is favored due to low-level mesoscale

Published online: 07 December 2010

convergence that lifts moist air, a necessary and key factor in the formation of a thunderstorm. In the presence of a synoptic scale disturbance, for example a frontal passage across a dryline, motion of a low-pressure area and the attendant upper-level trough may significantly affect the horizontal and vertical air motions along the dryline. In the absence of synoptic forcing, however, the storm is triggered solely due to convection.

Ground-based observations during the late afternoon of 22 May 2002 indicated that near-surface conditions were dominated by strong low-level convergence; hence, a dryline was formed between the location of the S-band dual Polarization Doppler Radar (S-Pol) and Homestead. Lidar-based observations at Homestead indicated a well-mixed convective boundary layer with the planetary boundary layer (PBL) height reaching about 3.6 km around 2130 UTC (Demoz et al. 2006). Although there was strong surface convergence, a well established and deep convective PBL, and strong upward air motion over the intensive observing region (IOR) on 22 May 2002, storm initiation did not occur. Storm initiation was wrongly predicted over this region by the National Oceanic and Atmospheric Administration (NOAA) Forecast System Laboratory-Rapid Update Cycle (FSL-RUC), the fifth-generation Pennsylvania State University-National Center for Atmospheric Research (NCAR) Mesoscale Model (MM5), and the National Center for Environmental Prediction (NCEP) Meso Eta models. Convection initiation occurred instead over northwest Kansas, far north along the dryline, late in the afternoon.

Previous studies have suggested several hypotheses to explain the lack of convection initiation in dryline events. The conceptual understanding of deep convection along the dryline was advanced by Ziegler and Rasmussen (1998), who suggested that strong shear within the boundary layer enhances entrainment and turbulent mixing between a cumulus cloud and its environment, diluting the buoyancy of the cloudy updraft. They also discuss ways in which moist boundary layer air parcels must be lifted to their lifting condensation level (LCL) and level of free convection (LFC) prior to leaving the mesoscale updraft to form deep convection. Their analysis has led to improvements in the conceptual model of dryline morphology. However, they noted a lack of detailed observations of the temporal and spatial variability of moisture and boundary layer height to properly test their ideas. In a study of the synoptic-scale environment of a dryline over the Texas panhandle on 6 May 1995, Richter and Bosart (2002) argued that a short-wave ridge over a dryline convergence zone was a cause for the absence of deep convection initiation. Cai et al. (2006) suggested that a weakening updraft due to weak baroclinic instability across the dryline, together with a strong capping inversion was one of the reasons why convection did not trigger over the Oklahoma panhandle during a dryline event on 11 June 2002. Weiss and Bluestein (2002) noted the key role played by a dry layer between the LCL and LFC above the convective boundary layer in inhibiting convection initiation in a dryline over the Texas panhandle on 3 June 1995; a similar phenomenon was also reported by Demoz et al. (2006) during the 22 May 2002 dryline study.

Although many studies have contributed to improvements in the general understanding of the formation and evolution of the dryline over the SGP, our understanding of the role of the water vapor distribution in convective initiation associated with the dryline is not completely clear. This is mainly due to the lack of complete, accurate, and high spatial and temporal resolution water vapor measurements. This was one of the motivations for the International H_2O Project, IHOP_2002 (Weckwerth et al. 2004), which has produced the most detailed and high-quality integrated measurement datasets to date. Making use of these measurements, several observation-based studies of the dryline on 22 May 2002 have been carried out. For example, Weiss et al. (2006) used finescale radar observations to indicate an area of concentrated subsidence away from the dryline convergence zone, potentially significant for the observed double dryline. They also reported a maximum upward vertical velocity of about 8.0–9.0 ms^{-1} over the dryline convergence zone. Using mobile ground-based radar and in situ meteorological data, Buban et al. (2007) noted the formation of small-scale vortices (misocyclones) along the dryline. These small-scale vortices are believed to influence convection initiation processes by augmenting the moisture and convergence fields, perhaps by enhancing vertical moisture fluxes. In another observational study, Demoz et al. (2006) argued that relatively low near-surface moisture values, together with a strong capping inversion and moisture detrainment between the LCL and the LFC, related to the overriding drier air, were critical for lack of convection initiation during the dryline on 22 May 2002. Wakimoto and Murphey (2009) found a tendency of maxima of a total derivative of radar reflectivity to be near regions where cumulus clouds developed near the dryline convergence. Their analysis of a series of soundings indicates that the maximum height of the surface-based parcels is far below the height of the LFC.

In order to have a better understanding of the role played by boundary layer moisture and to understand the possible reasons for the lack of storm initiation over the IOR despite the strong upward lift and well-mixed boundary layer, a thorough investigation of boundary layer moisture evolution and variability during the dryline on 22 May 2002 is conducted in this study. The moisture investigation in this study is much more complete than in the other studies. Moisture evolution and structure during 22 May is

compared with other convective and non-convective dryline cases during the IHOP_2002 time period. In addition, we also present a detailed comparison of the observed water vapor variability to simulation results using different numerical models and investigated the model's wrong prediction of storm initiation that did not occur in reality. The scientific objective of this paper is to understand the boundary layer processes that contribute to the lack of convection initiation. In particular, the study tests the hypothesis that beyond the lifting mechanism, a sustained and abundant moisture profile in the boundary layer is required for convection initiation to occur along a dryline.

The prevailing meteorological conditions over the Oklahoma–Texas panhandle area during the 22 May 2002 dryline case are presented in Sect. 2. Section 3 deals with the observational data used in the current study. Results of the observational analysis of boundary layer moisture evolution and structure during the non-convective dryline on 22 May 2002 compared to convective dryline cases are presented in Sect. 4. The analyses of the evolution of the observed boundary layer height, the moisture representation in numerical models and the convective available potential energy (CAPE) and convection inhibition (CIN) are also included in Sect. 4. Section 5 gives a brief summary and conclusions.

2 Environmental conditions

The near-surface environment on 22 May 2002 was characterized by the convergence of moist southeasterly and dry southwesterly winds over the Oklahoma and Texas panhandles. The boundary between these two large-scale flows was oriented southwest/northeast and a late afternoon dryline was formed between S-Pol and Homestead in the Oklahoma Panhandle. In situ observations indicated abrupt changes in moisture, temperature and wind direction as the dryline passed over the site around late afternoon, 2130 UTC (UTC = Central Daylight Time (CDT) + 5 h) (Demoz et al. 2006). Near-surface mixing ratio values increased with time due to northward moisture advection (Weiss et al. 2006). A visible image from the Geostationary Operational Environmental Satellite (GOES) (see Fig. 1 of Demoz et al. 2006 and Fig. 5 of Weiss et al. 2006) shows a wedge-shaped area of scattered cumulus cloud over the Oklahoma and northern Texas panhandles. The NCAR S-Pol radar data (not shown) indicated a double-fine-line structure around 2300 UTC where the double dryline was established over the wedge-shaped area of cumulus clouds (e.g., Demoz et al. 2006; Wakimoto and Murphey 2009).

There was no significant synoptic forcing over the IOR during the day. However, the upper air pattern was characterized by a long-wave trough tilting from northwest to southeast and propagating eastward through the day. Using radar, in situ, and Lagrangian analysis, Buban et al. (2007) reported the presence of misocyclones propagating from north-to-south along the dryline. These misocyclones were distorting the moisture fields over the dryline convergence zone (Wakimoto and Murphey 2009). No convection initiation took place in the IOR during this period. However, deep convection was reported late in the afternoon farther north along the dryline, a region that could have been influenced by the upper air trough. The 22 May 2002 dryline is generally stronger in terms of humidity contrast and confluence than the other drylines during IHOP_2002 (Miao and Geerts 2007). Detailed discussion on the environmental conditions during the dryline on 22 May 2002 can be found in Weiss et al. (2006), Demoz et al. (2006) and Buban et al. (2007).

3 Data sources

Observational datasets used in the study were obtained from the International H_2O Project (IHOP), a multi-agency observational field campaign that targeted the U.S. Southern Great Plains in summer 2002. During this field project a comprehensive suite of operational and research instruments were deployed over the IOR near the Oklahoma and Texas panhandles. A detailed discussion on IHOP_2002 experimental design and instrumentation can be found in Weckwerth et al. (2004). The current research has taken advantage of the unique high spatial and temporal resolution dataset obtained from the extensive measurements of the first dedicated convection initiation mission of the IHOP project during the dryline on 22 May 2002. The measurements used in this study included the National Aeronautics and Space Administration (NASA) Goddard Space Flight Center (GSFC) Lidar instruments, i.e., Scanning Raman Lidar (SRL) and the Holographic Airborne Rotating Lidar Instrument Experiment (HARLIE); ground-based Atmospheric Emitted Radiance Interferometer (AERI); National Center for Atmospheric Research-Integrated Sounding System (NCAR-ISS); and radiosondes from the National Weather Service (NWS). Field reports as well as operational and research model products from the IHOP_2002 data catalog were also used to investigate boundary layer moisture structure and evolution along the May 22 dryline.

4 Results

A better understanding of the dynamic and thermodynamic processes in the dryline environment is crucial in determining the timing and location of convection initiation. In

boundary layer thermodynamic processes, the distribution of water vapor plays a significant role. Unlike temperature and horizontal wind fields, atmospheric moisture varies significantly over small space and time scales. Due to this variability, measurements made with commonly used radiosondes do not provide adequate resolution in space and time and can make significant errors (as large as 1.0 g kg^{-1}) in water vapor mixing ratio (Weckwerth et al. 1996; Demoz et al. 2006). These errors are important because past simulation studies have indicated sensitivity of thunderstorm initiation to slight changes in the input moisture profile from radiosondes (Crook 1996). Therefore, the accurate and high temporal and spatial resolution water vapor mixing ratio measurements during IHOP_2002 are necessary for studying the moisture distribution that permits dryline convection initiation.

Among the important factors that need to be considered when studying the role of moisture in convection initiation due to a dryline event include the amount of available moisture and sustainability of the supply of moisture. The latter requires a critical look at the temporal evolution of moisture. In the following sections we present results of the 22 May 2002 observational moisture analysis. Abundance, depth and sustainability of the moisture supply during this day and other relevant dryline cases are discussed. Simulated boundary layer mixing ratio values were also compared with the observations.

4.1 Temporal evolution of moisture

In an attempt to determine the role of boundary layer moisture in dryline convection initiation, water vapor mixing ratio retrievals from AERI at Homestead site were analyzed. The moisture analysis includes comparison of the dryline event on 22 May to the dryline cases in the presence of synoptic forcing, and cases where convective storms were triggered due to the dryline in the absence of synoptic forcing, all during the IHOP_2002 campaign. The characteristics of the time periods considered here are summarized in Table 1. The surface moisture on 22 May was much lower compared to the convective and non-convective frontal dryline on 10 and 11 June 2002, respectively (Fig. 1a). The moisture jump followed by a large dip between 1830 and 2400 UTC 22 May is the result of the onset of the dryline and its subsequent back and forth movement over Homestead (Demoz et al. 2006; Wakimoto and Murphey 2009). Also shown in Fig. 1a) is a significant moisture decrease after 2100 UTC on 11 June that indicates a weakening dryline (Cai et al. 2006).

A study carried out by Wilson and Roberts (2006) indicate five cases (24 and 27 May; 12, 15, and 19 June 2002) of convection initiation triggered due to the dryline, in the absence of synoptic forcing, over the Oklahoma and Texas panhandles during IHOP_2002. With the exception of 24 and 27 May (for which data is missing), a time series plot of AERI surface water vapor mixing ratio during these convective dryline cases (Fig. 1b) revealed persistent and abundant moisture as compared to 22 May. The surface moisture plots show that the 22 May case was different from most of the other cases in two major ways: (1) The trend of moisture was progressively increasing throughout the day from a very dry value of $\sim$5.0 g kg^{-1} to an average value of about 8.0–9.0 g kg^{-1} in the afternoon (except around 1700 UTC); (2) The mixing ratio values were lower than all the other cases and were below 9.0 g kg^{-1}, a value which has significance as a lower threshold for thunderstorm initiation (Schaefer 1986). At 2100 UTC (4:00 p.m. local), a time when most storms initiate in the region, the surface moisture plot reveals a deficit of 2.0 g kg^{-1} or more on 22 May compared to the others. This significant mixing ratio difference between 22 May and the rest of the convective dryline cases indicates the lack of abundant surface moisture on 22 May. This inadequate surface moisture could be one of the reasons for the lack of convection initiation during the dryline on 22 May.

The same moisture analysis as in Fig. 1a, b, but at 2.0 km above ground level (AGL) is shown in Fig. 1c, d. At this higher level water vapor mixing ratio values were comparable for part of the time in most of the cases, with a noticeably increasing trend after 1900 UTC on 22 May (Fig. 1c, d). This increase in moisture at 2.0 km AGL indicates the strength of convection in the boundary layer at a time when the dryline on 22 May became

Table 1 Water vapor mixing ratio retrievals from AERI at Homestead during the IHOP_2002 dryline cases

Cases in IHOP_2002	Convective	Synoptic forcing	Mixing ratio (g kg^{-1})	
			Surface	2 km AGL
22 May	No	No	8.2	2.9
10 June	Yes	Yes	13.1	4.0
11 June	No	Yes	10.3	5.0
12 June	Yes	No	10.1	1.5
15 June	Yes	No	12.0	6.4
19 June	Yes	No	10.5	2.7

Mixing ratios are time average between 1600 and 2400 UTC at the surface and 2 km AGL

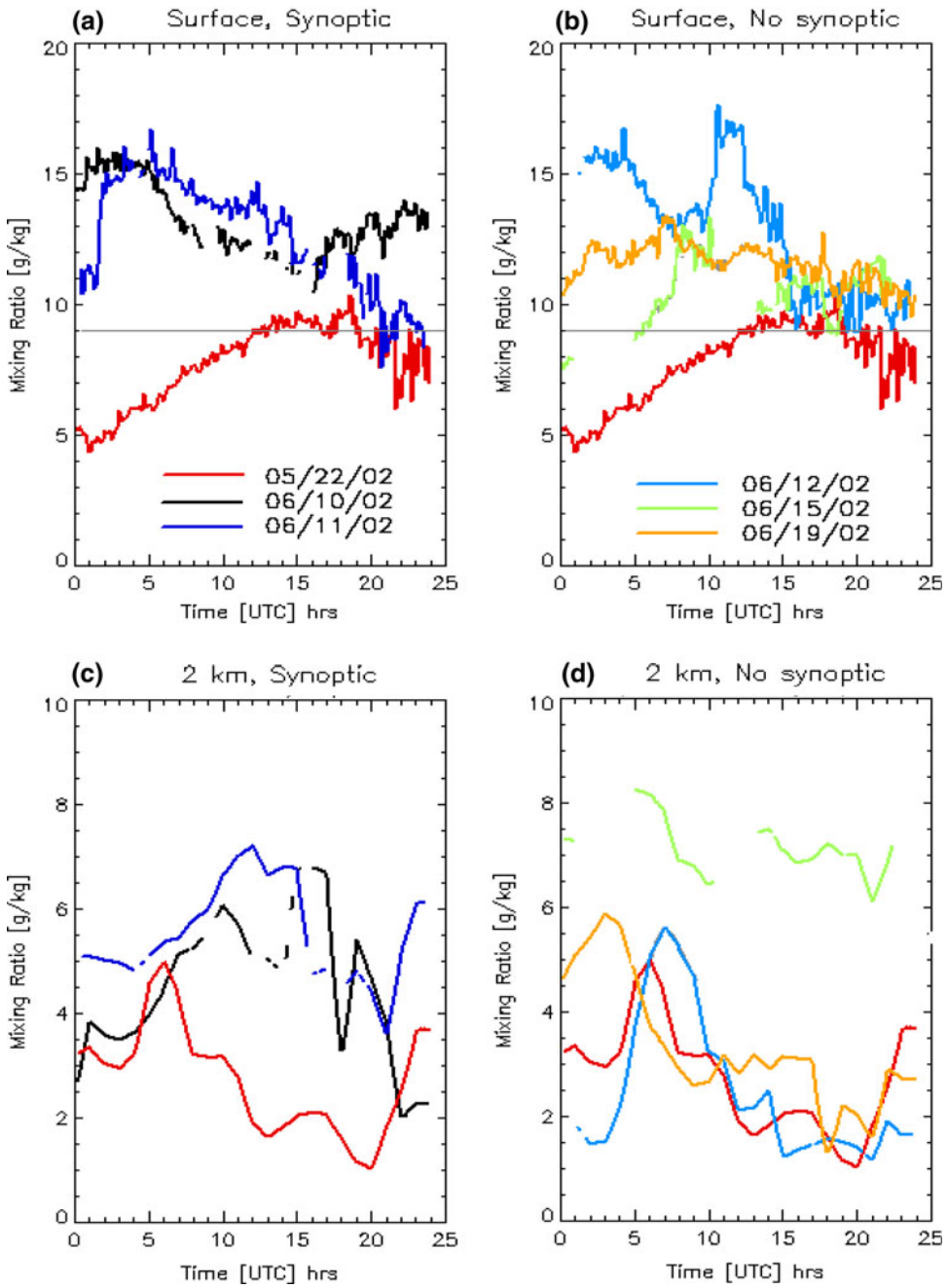

Fig. 1 Comparison of time series of AERI water vapor mixing ratio at Homestead: **a** 22 May 2002 compared to synoptic cases at surface; **b** 22 May 2002 compared to five convective dryline cases, non-synoptic at surface; **c** same as in **a** but at 2 km above ground level; **d** same as in **b** but at 2 km above ground level. The 9.0 g kg^{-1} mixing ratio value, a lower threshold for thunderstorm initiation (Schaefer 1986), is indicated by the *horizontal line* in the *top panels*

well-pronounced. In the absence of synoptically forced upward motion, the storm is triggered solely due to convection. Compared to the dryline cases with synoptic forcing (Fig. 1c) and those in the absence of synoptic forcing (Fig. 1d), moisture at 2.0 km level on 22 May was not substantially lower. The deficit of low-level moisture together with the relatively abundant moisture at 2 km AGL suggests that the dryline was characterized by strong convective activity. In an observation-based study, strong vertical velocity ($\sim$8–9 m s^{-1}) was reported in the boundary layer during 22 May (Weiss et al. 2006). Note that the increase in moisture at 2.0 km cannot be explained by horizontal advection, as winds at 2.0 km were from the drier region, west of Homestead, Oklahoma.

Time–height plots of AERI water vapor mixing ratio indicate low moisture in the boundary layer early on the day, followed by a relative increase in moisture after 1700 UTC, local noon on 22 May (Fig. 2a). However, more moisture surge occurred over the Homestead area, late at night (not shown) when the active convection started to dampen, as discussed later in Sect. 4.2. In contrast to the 22 May case, the convective dryline on 10 June (Fig. 2b) was characterized by an abundant ($\sim$12.0 g kg^{-1}), deep, and sustained supply of moisture. This boundary layer

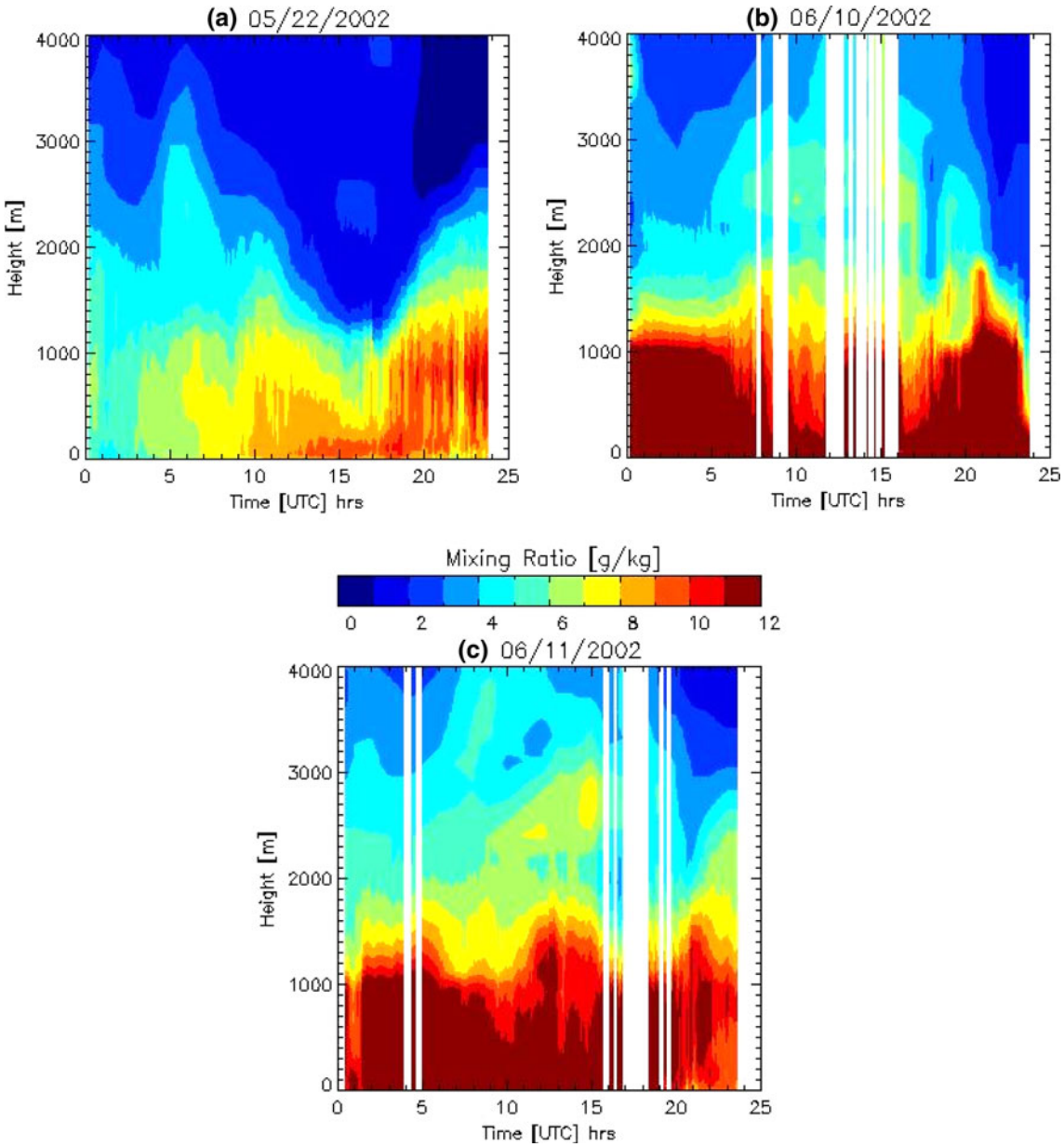

Fig. 2 Time–height plot of AERI retrieved water vapor mixing ratio at Homestead, OK. **a** 22 May 2002; **b** 10 June 2002; and **c** 11 June 2002. *The vertical white lines* (mixing ratio gaps) in **b** and **c** mark the missing data

moisture, in combination with a cold frontal boundary forcing (i.e., the source of updraft and vertical shear), played a significant role in storm initiation on 10 June 2002. During this period, misocyclones associated with vertical velocity maxima were reported by Arnott et al. (2006). In the higher temporal resolution SRL lidar data (not shown), a spike in water vapor mixing ratio was noted at 2300 UTC that was caused by a propagating thunderstorm outflow boundary from the south west of the Homestead site (Demoz et al. 2006). The effect of this propagation cleared moisture at the Homestead profiling site temporarily near 0000 UTC.

A similar moisture analysis of the 11 June 2002 IHOP case (discussed in detail by Cai et al. 2006) is also shown for comparison in Fig. 2c. In this case a mixing ratio value of about 12 g kg^{-1} persisted in the lower boundary layer from the earlier convective day up to local noon on 11 June 2002. Moisture deceased significantly throughout the boundary layer late in the afternoon. No convection was triggered in the Oklahoma panhandle region on this day. Note, however, that a significant increase in moisture occurred during the night when convective activity was absent and mid-level subsidence was present. In fact, the increase in moisture continued further into the afternoon

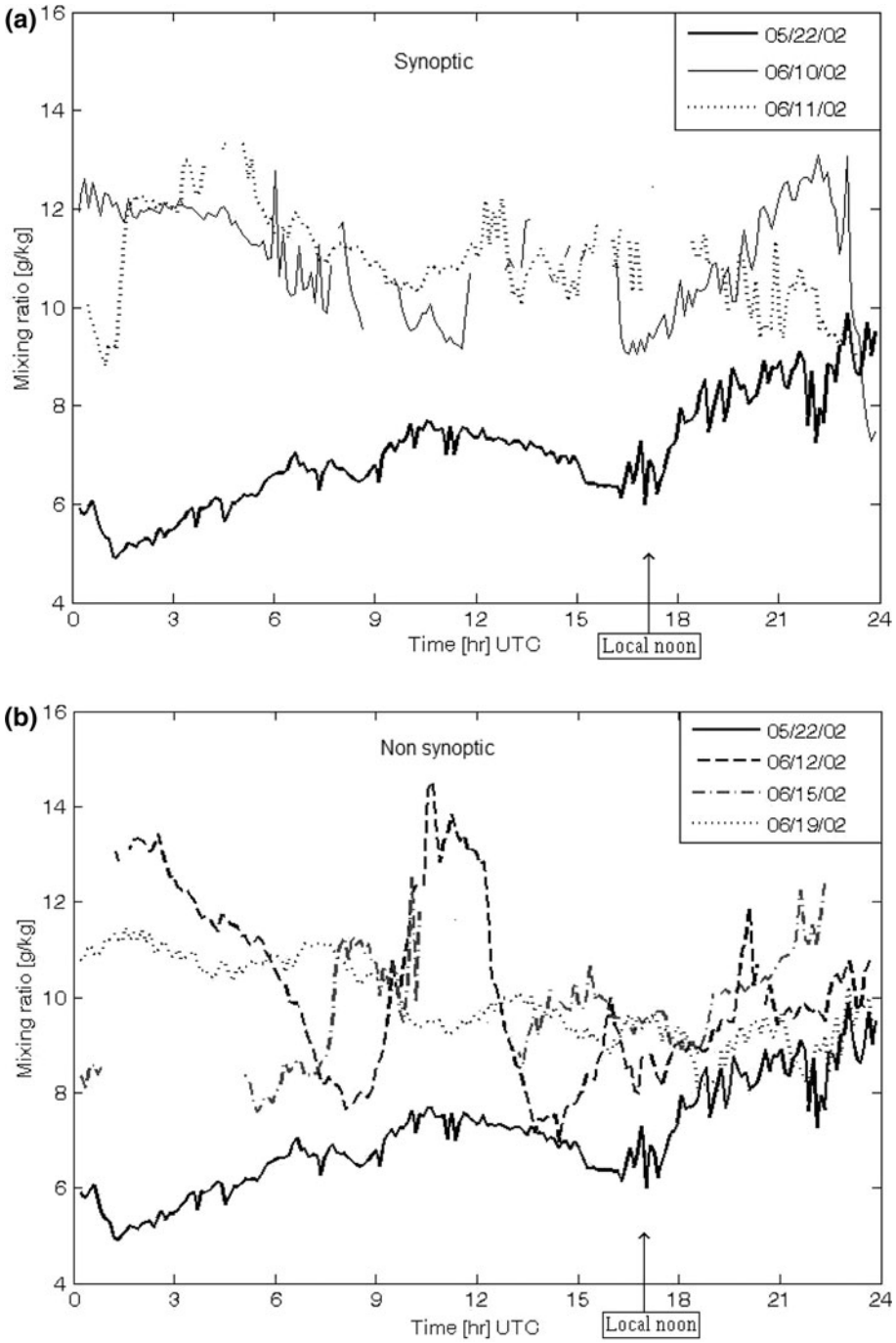

Fig. 3 Surface-to-2 km averaged AERI water vapor mixing ratio at Homestead: **a** 22 May compared to 10 and 11 June, and **b** 22 May compared to four convective dryline cases

where convection initiation was observed near Homestead on 12 June (Markowski et al. 2006).

To further investigate the boundary layer moisture, the surface to 2 km AGL averaged water vapor mixing ratio on 22 May was analyzed to compare with the dryline cases likely influenced by synoptic forcing (Fig. 3a), as well as those in the absence of major synoptic forcing (Fig. 3b). Two important points are revealed from the data: (1) the 22 May surface to 2 km AGL average water vapor mixing ratio value was the lowest in magnitude compared to the other cases, which is similar to what is discussed above, and (2) the afternoon moisture trend for 22 May and 10 June are increasing, unlike that of 11 June. The increase in the averaged moisture is a result of the active moistening of the boundary layer by convection. This suggests that the deficit of low-level moisture was the main cause for the lack of convection initiation on 22 May. A summary of average mixing ratio at the surface and 2 km AGL during 22 May and the convective IHOP_2002 dryline cases is shown in Table 1. The average surface mixing ratio

between 1600 and 2400 UTC at Homestead reveals the persistence of abundant (10–12 g kg^{-1}) moisture on 12, 15, and 19 June, all of which are convection initiation cases with the dryline located over Homestead. Compared to the aforementioned three dryline cases, the average surface moisture on 22 May was low. At 2 km AGL the average mixing ratio on 22 May was comparable to 19 June; and is larger than the 12 June case at the same level.

4.2 Vertical structure of moisture

The vertical moisture structure during dryline events is analyzed using the water vapor mixing ratio derived from the NCAR-ISS soundings at Homestead site (Fig. 4). Radio sounding data between 1900 and 2100 UTC is used for comparison and we have separated these sounding profiles into days where the dryline occurred with strong synoptic influences (10 and 11 June) (Fig. 4b) and cases where the dryline occurred in the absence of strong synoptic influences near Homestead (Fig. 4a). Note that complete time–height plots of the moisture can be used to discuss the boundary layer moisture structure/evolution in detail. Radiosonde data are used in this analysis because of the (availability of data for all the dryline cases considered) high temporal sampling. Despite the higher measurement errors, the radiosonde data analysis is consistent with the previous results in Sect. 4.1, i.e., that moisture was neither deep nor plentiful on 22 May, compared to the 10 and 11 June cases. It should be noted that although moisture was deep and plentiful on 11 June case, there was no storm initiation in the day due to: weak updrafts; a substantial dry layer between the LCL and LFC; and strong cap inversion as a result of middle-level subsidence over the Oklahoma panhandle (Cai et al. 2006). Below 3.0 km AGL, the 22 May average mixing ratio value was 8.5 g kg^{-1}; 5.0 and 3.0 g kg^{-1} less compared to the 10 and 11 June cases, respectively. Sounding profiles above 3 km AGL for the three cases show a significant decrease in moisture as expected, with 22 May and 11 June being an average of 1.0 g kg^{-1} ($\sim$radiosonde error) drier. Above 5.5 km AGL, mixing ratio values on 11 June (not shown) increased due to moisture advection to the IOR. This advection was due to an upper trough, located further northwest of the IHOP domain, which extended from an upper low centered over eastern Montana and the Canadian border (e.g., Cai et al. 2006). A comparison of the moisture structure on 22 May with other dryline cases later in the IHOP_2002 season also revealed similar conclusions that the boundary layer on 22 May was the driest of all the dryline events that occurred during the campaign.

The above results suggest that in the absence of synoptic forcing, abundant planetary boundary layer moisture is one of the required ingredients for convection initiation, in addition to instability and upward vertical motion. Except for 24 May, all other cases where dryline convection was triggered in the absence of synoptic forcing had water vapor mixing ratio values $\geq$10.0 g kg^{-1} throughout the boundary layer (Fig. 4b). The exceptional case of 24 May can perhaps be explained by the presence of a triple point east of Homestead (Wakimoto et al. 2006). This triple

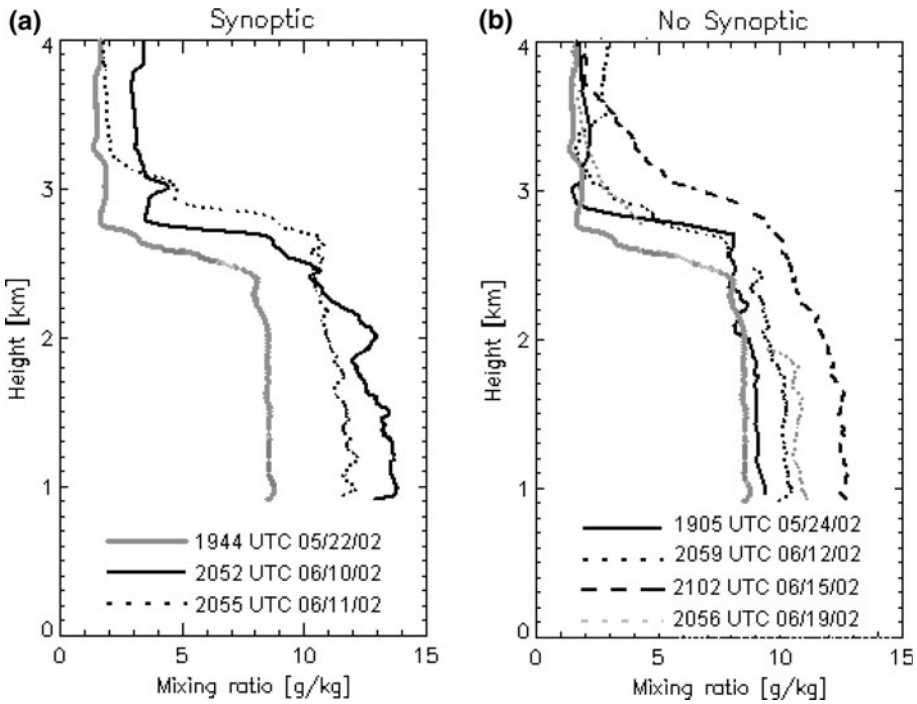

Fig. 4 Vertical structure of mixing ratio derived from NCAR-ISS soundings, Homestead: **a** 22 May compared to 10 and 11 June, and **b** 22 May compared to four convective dryline cases

point, combination of a surface low, warm front and dryline, is a favorable area for severe thunderstorm development.

In summary, we have shown that on 22 May the water mixing ratio profile over the Homestead site was not deep, and abundant moisture did not sustain in the afternoon when most convection initiates. However, the day was characterized by very strong humidity contrast and convective activity. Compared to the 10 June case, where convection initiation was observed near the site, moisture throughout the boundary layer was 40% less on 22 May. An interesting case is the 11 June, null-convection initiation, where the moisture amount was somewhat higher than 22 May, but much lower than the 10 June case. We hypothesize that the lack of persistent and abundant surface moisture (Fig. 1b) is one of the main reasons that the 22 May dryline failed to trigger convection over the IOR. The strong relationship between convective turbulence and height of the planetary boundary layer (PBL), i.e., the convective boundary layer (CBL), is sometimes used to define the boundary layer. In Sect. 4.3 we consider the height of the boundary layer and its characteristics during the dryline events.

4.3 Planetary boundary layer height

Time–height plots of PBL height derived from HARLIE, a scanning aerosol backscatter lidar instrument of the NASA/GSFC (Schwemmer 1998), for three dryline cases (22 May, 10 and 11 June 2002) are shown in Fig. 5a. HARLIE uses a holograph with a 45° diffraction angle and rotates continuously in Azimuth during its operation resulting in a conical scan of data at 20 m vertical sampling. During IHOP_2002, a scan rate of 30°/s (360/30 = 12 arcs on the surface of a con centered at the surface) was used. The PBL height for each of the 12 profiles per scan is derived from the backscatter profiles and the plotted PBL height is the average of the 12 scans. The standard deviation of the heights is also derived as a measure of the variability around the average. Comparisons of HARLIE-derived PBL heights with other lidars and sonde (Miiller et al. 1999) indicate that HARLIE typically overestimates PBL height by about 200 m.

The PBL heights, as measured by HARLIE, increased continuously, reaching about 4 km AGL on 22 May (Fig. 5a). This result indicates the largest rate of growth as well as the deepest PBL height compared to both the convective 10 June as well as to the non-convective 11 June dryline cases. Although much lower in depth, the general trend of the PBL height on 10 June is similar to that of 22 May. On 11 June, however, a decrease in the PBL height was observed starting at 2200 UTC. This decrease may be related to the strong capping inversion and very dry layer of air above the PBL—as is usually the case when a stratospheric intrusion occurs. What is most interesting is that the 22 May case showed the largest PBL height growth rate compared to the 10 and 11 June cases. In fact, the measured PBL height on 22 May was the deepest in the entire IHOP_2002 dataset.

As mentioned above, HARLIE also measures the standard deviation of the PBL heights at each scan. These values are a measure of how variable the PBL height was from one scan to the next, hence, a direct measure of the activity of the boundary layer convection. The variability data plot (Fig. 5b) reveals that the PBL heights on 22 May case were highly variable from scan to scan, as were the values from 10 June 2002. Note that the peak between 2300 and 2330 UTC on 10 June was a result of a thunderstorm outflow that affected the lidar profiling site. Comparatively, except for the period of the thunderstorm outflow on 10 June, the PBL variability overall was larger on 22 May 2002. In summary, the HARLIE-derived PBL heights and scan-to-scan variability reveal that the boundary layer convection on 22 May was vigorous and deep.

4.4 Convective available potential energy and convection inhibition

A high value of convective available potential energy (CAPE) and reduced convection inhibition (CIN) are among the conditions necessary for severe storm initiation (Weckwerth and Parsons 2005). A Skew-t plots of the NCAR-ISS soundings (Fig. 6) show CAPE/CIN values of 683/-207, 2319/-99, and 1132/-111 J kg^{-1} on 1944 UTC 22 May, 2055 UTC 10 June and 2055 UTC 11 June 2002 cases, respectively. The relatively high value of CAPE-to-CIN ratio for 22 May and 11 June would have been a factor for the initiation of convection. However, the airmass over stations to the immediate east of Homestead on 22 May was characterized by appreciable CAPE (CAPE = 1,281 J kg^{-1}; CIN = −214 J kg^{-1}), higher dew point temperatures at low-levels, and an abrupt drying of the air above (Demoz et al. 2006). Note that the 10 June case, which had the largest and deepest boundary layer moisture, also had the largest CAPE. To investigate this further, temporal evolution of CAPE and CIN values derived from AERIplus (Feltz et al. 2003) retrievals at Homestead between 1800 and 2400 UTC on 22 May, 12, 15 and 19 June 2002 are shown in Fig. 7. On 22 May, the CAPE values exceed 2000 briefly just after the passage of the dryline as compared to the consistent 1500+ CAPE values on the other dryline convection days of IHOP_2002. As indicated in the vertical moisture structure (cf., Fig. 4b), these convective dryline cases with relatively high CAPE values are characterized by abundant and deep water vapor mixing ratios (≥10.0 g kg^{-1}) in the boundary layer.

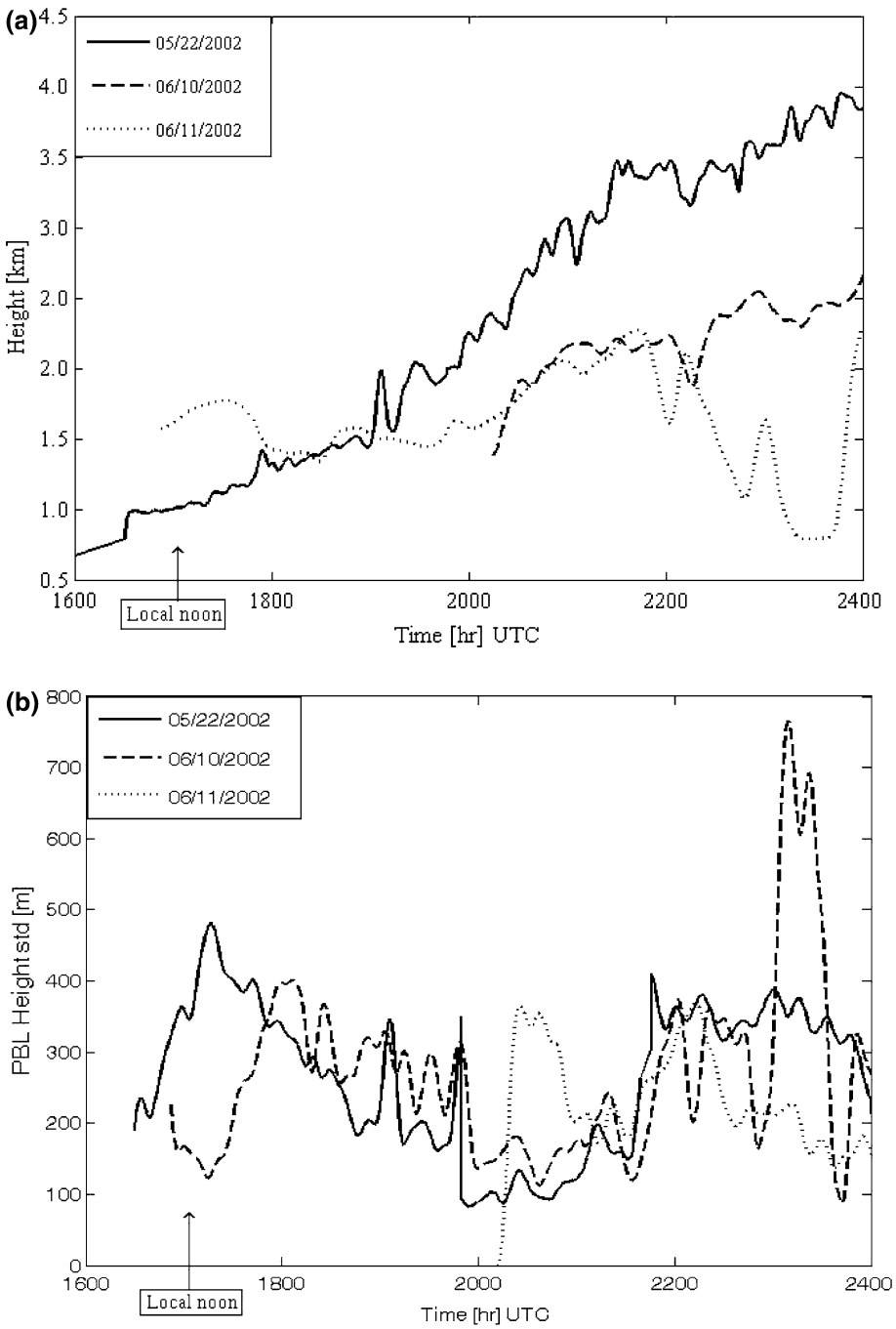

Fig. 5 Lidar-based HARLIE observation. **a** PBL height, and **b** PBL Height standard deviation at the Homestead profiling site

To further investigate the impact of moisture in CAPE and CIN computations, the following hypothesis was examined. From the surface up to the 700 mb pressure level the water vapor mixing ratio in the 1944 UTC 22 May sounding profile was increased by 20%. The corresponding dew point temperature was then calculated, keeping the temperature constant, resulting in modified CAPE and CIN values. The result (Table 2) reveals that a 20% increase in boundary layer moisture on 22 May resulted in a 100% increase in CAPE and a 40% decrease in CIN. A 40% increase in boundary layer moisture increases CAPE by a factor of 3 and decreases CIN by a factor of 4. This underscores the importance of the quality of the moisture information on the variables necessary for convection initiation. In Sect. 4.5, we present a brief discussion of the simulated boundary layer moisture for 22 May using different models and compare them with the observations. A more detailed investigation of the effect of

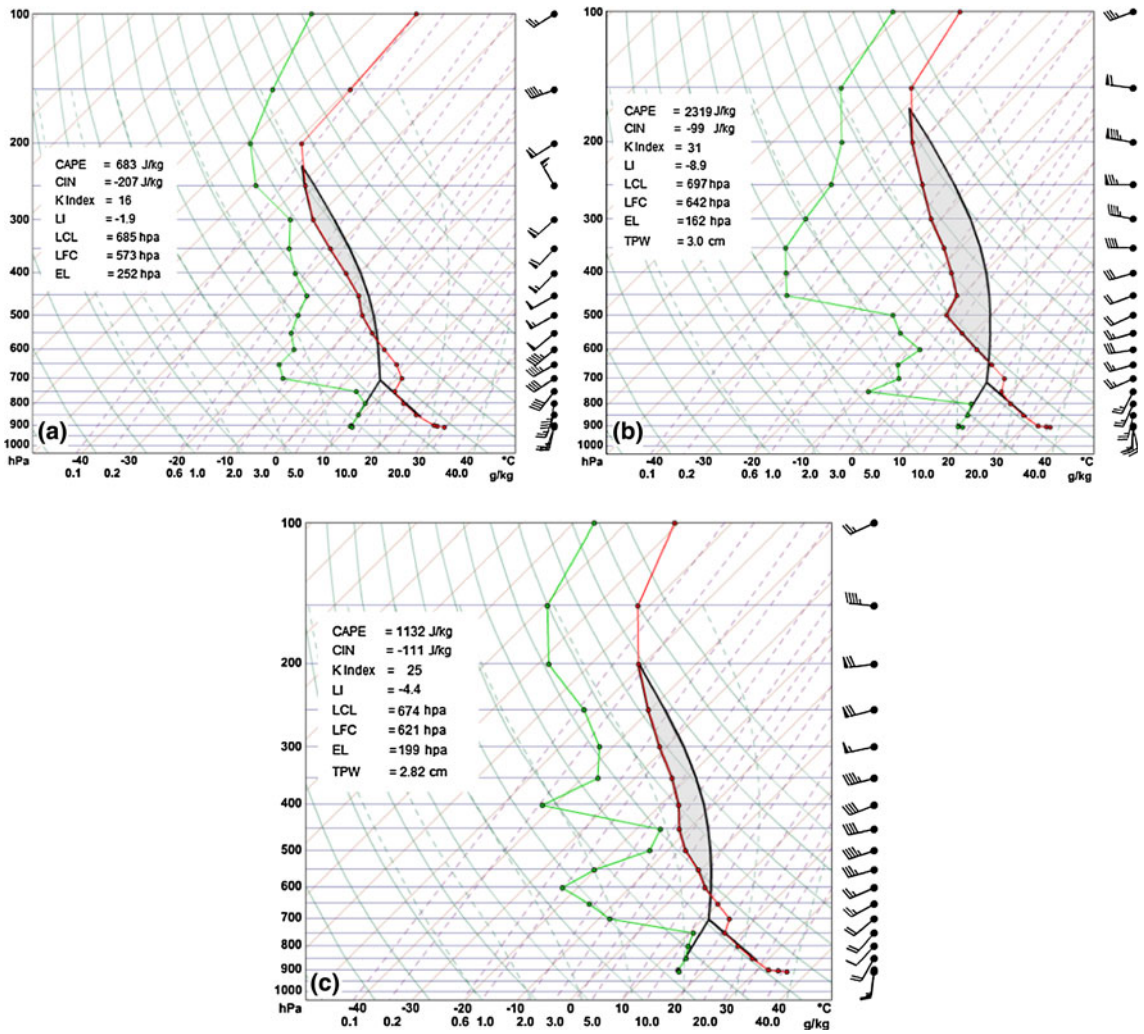

Fig. 6 Skew-t plots for convective and non-convective dryline cases at Homestead from NCAR-ISS soundings. **a** 1944 UTC 22 May; **b** 2055 UTC 10 June; and **c** 2055 UTC 11 June 2002

modifying the moisture in WRF initialization and the resulting detailed vertical and horizontal moisture stratification on convection initiation forecast is beyond the scope of this paper and will be presented in a separate paper.

4.5 Moisture representation in numerical models

Several operational and research forecast models, such as MM5, wrongly predicted the presence of storm initiation over Oklahoma panhandle during the 22 May 2002 dryline. There could be several reasons why these numerical models wrongly predicted the presence of storm initiation over Oklahoma panhandle on 22 May 2002, which was not present in reality. A detailed discussion on modeling of the 22 May 2002 dryline is beyond the scope of this paper; however, using the unique and extensive IHOP measurements we wanted to make a brief comparison assessment of the simulated boundary layer moisture from numerical models with the observations. The objective of this section is to possibly explain why the numerical models wrongly predicted the presence of storm initiation on 22 May 2002.

In the absence of strong synoptic influences, as in the case of 22 May 2002, motion of the dryline during the day is mainly controlled by vertical mixing processes in the PBL. The vertical turbulent transport of moisture and heat within the PBL are sub-grid processes and therefore are parameterized in modeling study. Different PBL parameterization schemes have different description of the vertical mixing processes that lead to different simulation results (e.g., Wisse and De Arellano 2004; Trier et al. 2004). For example surface heating and boundary layer mixing were found to be responsible for the general deepening of the boundary layer on 24 May 2002 dryline (Xue and Martin 2006). Qualitative precipitation forecasts with parameterized convection require an accurate representation of the spatial and temporal water vapor distribution (Perkey 1976;

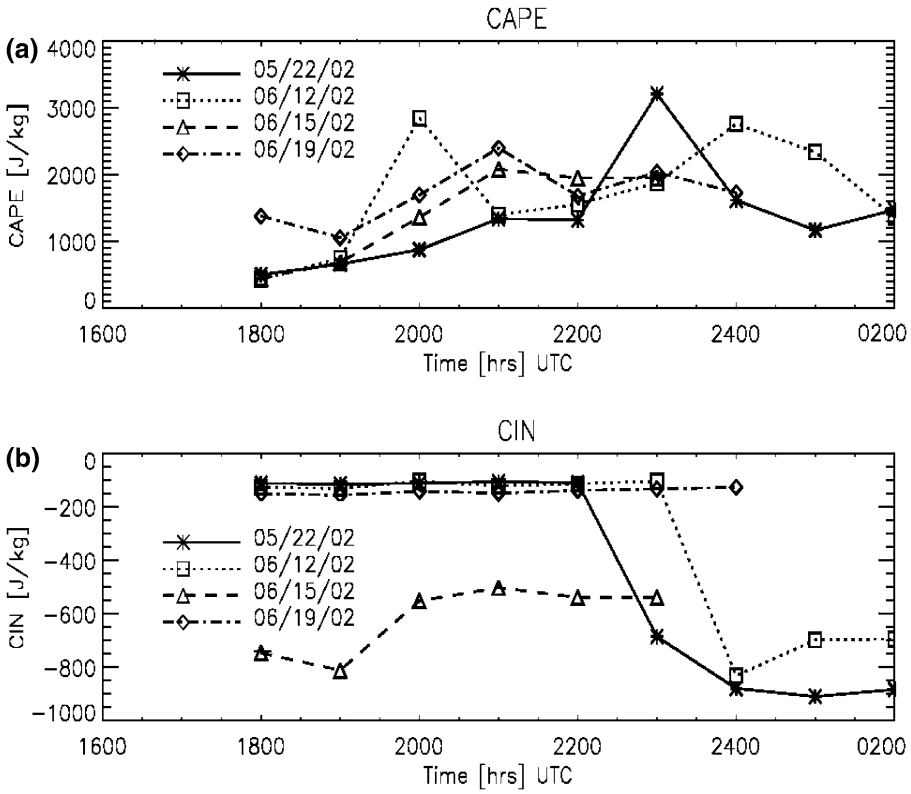

Fig. 7 Time series plots of **a** CAPE (J kg^{-1}), and **b** CIN (J kg^{-1}) values at the Homestead profiling site from AERIplus. Note that in all of the cases the dryline was over the profiling site between 2130 and 2230 UTC

Table 2 Computed CAPE and CIN values using Skew-T diagram as a result of surface-to-700 mb mixing ratio increase in the sounding profile at Homestead

(J kg^{-1})	Mixing ratio increase in percentage								
	0	5	10	15	20	25	30	35	40
CAPE	683	781	928	1,128	1,396	1,625	1,792	1,978	2,211
CIN	−207	−192	−171	−146	−121	−98	−82	−65	−44

The computation was made from NCAR-ISS 1944 UTC 22 May 2002 sounding

Mills 1983; Mailhot et al. 1989; Kock and Clark 1999). In cloud resolving models, a correct prediction of convection is dependent on accurate estimates of water vapor distribution within the boundary layer (Crook 1996). In this section we investigate how the boundary layer moisture is represented on the 22 May 2002 dryline simulations using the Weather Research and Forecasting (WRF) model (Skamarock et al. 2001) in the current study and the NCAR/Penn State Fifth Generation Mesoscale Model (MM5) output obtained from IHOP_2002 data archives (http://www.eol.ucar.edu/projects/ihop/dm/).

The NCAR Advanced Research WRF (ARW) dynamic core was used for the WRF simulations which were performed over two nested domains centered over the Oklahoma panhandle. The two domains have 202 × 202 and 481 × 481 grid points with a corresponding horizontal resolution of 4.0 and 1.0 km respectively. Both domains were configured to have 50 unequally-spaced vertical levels. The Mellor-Yamada-Janjic boundary layer scheme (Mellor and Yamada 1982; Janjic 2002) and Purdue Lin microphysics (Lin et al. 1983; Chen and Sun 2002) were used. The atmospheric model is coupled to the Noah land-surface model (Chen and Dudhia 2001) that includes four soil layers and a moisture model with canopy moisture prediction. The initial and lateral boundary conditions for the simulations were provided by the National Center for Environmental Prediction (NCEP) operational Eta model. The MM5 ver-3 model was configured to have three nested domains centered over Homestead with a horizontal grid spacing of 12.0, 4.0, and 1.33 km. All three domains were configured to have 30 unequally-spaced vertical levels. The Blackadar boundary layer scheme (Blackadar 1979) was used for PBL parameterization. The atmospheric model in MM5 is coupled to a multi-layer soil scheme; and simple-ice microphysics scheme with explicit treatment of cloud water, rain water, snow, and ice was used in the

simulations. Simulations start at 1200 UTC 22 May 2002 and run for a period of 24 h.

The National Weather Service (NWS) sounding profiles in Fig. 8a show no significant boundary layer moisture variability over the IHOP domain at the start of the simulation, with fairly good Eta model agreement. The Eta derived water vapor mixing ratio values at Homestead are within 1.0 g kg^{-1} of the soundings from Amarillo (AMA), Texas, and Dodge City (DOD), Kansas, stations (Fig. 8a). This establishes that there was little difference between the initial moisture output from the Eta model and the sounding measurements, and we next look at the subsequent evolution of the moisture via the dynamics and physics of the MM5 and WRF models.

At 2100 UTC, the simulated boundary layer mixing ratio profiles over the Homestead site from WRF at 4-km horizontal grid-resolution is over-predicted by about 1.2 g kg^{-1}, while MM5 (same resolution as WRF) underpredicted moisture by 1.6 g kg^{-1} below the 750 mb level (Fig. 8b). Note we have used the radiosonde launched at a somewhat earlier time of 1944 UTC 22 May for comparison, assuming that changes over one hour are small since the boundary layer is well-mixed – changes will be small if there is little horizontal variability in the water vapor field. Above the 750 mb level, WRF agree relatively well with the observations, however, the mixing ratio values from MM5 is much larger compared to the observations and that of WRF. This is a likely consequence of the Blackadar scheme in MM5 that uses a nonlocal approach in PBL parameterization compared to the MYJ scheme in WRF, which uses a local approach with a prognostic turbulent kinetic energy. The Blackadar scheme is known to produce nearly well mixed boundary layer during the daytime (Braun and Tao 2000; Wisse and De Arellano 2004). The output from Eta (40 km resolution) underestimated mixing ratios in the boundary layer by $\sim$3.0 g kg^{-1}.

In order to evaluate the effect of model spatial resolution on the accuracy of the simulated moisture profile, WRF was run at 1-km horizontal resolution. Increasing the horizontal grid resolution in WRF model from 4 to 1 km resulted in a 0.6 g kg^{-1} decrease in the mixing ratio values, hence, improvements of model performance compared to 4-km resolution below 750 mb. However, there is no significant change in moisture above 750 mb compared to the 4-km resolution (Fig. 8b). Both MM5 and Eta models overestimated moisture above the 750 mb level. In general WRF with MYJ scheme, and higher order advection and temporal integration schemes (Wicker and Skamarock

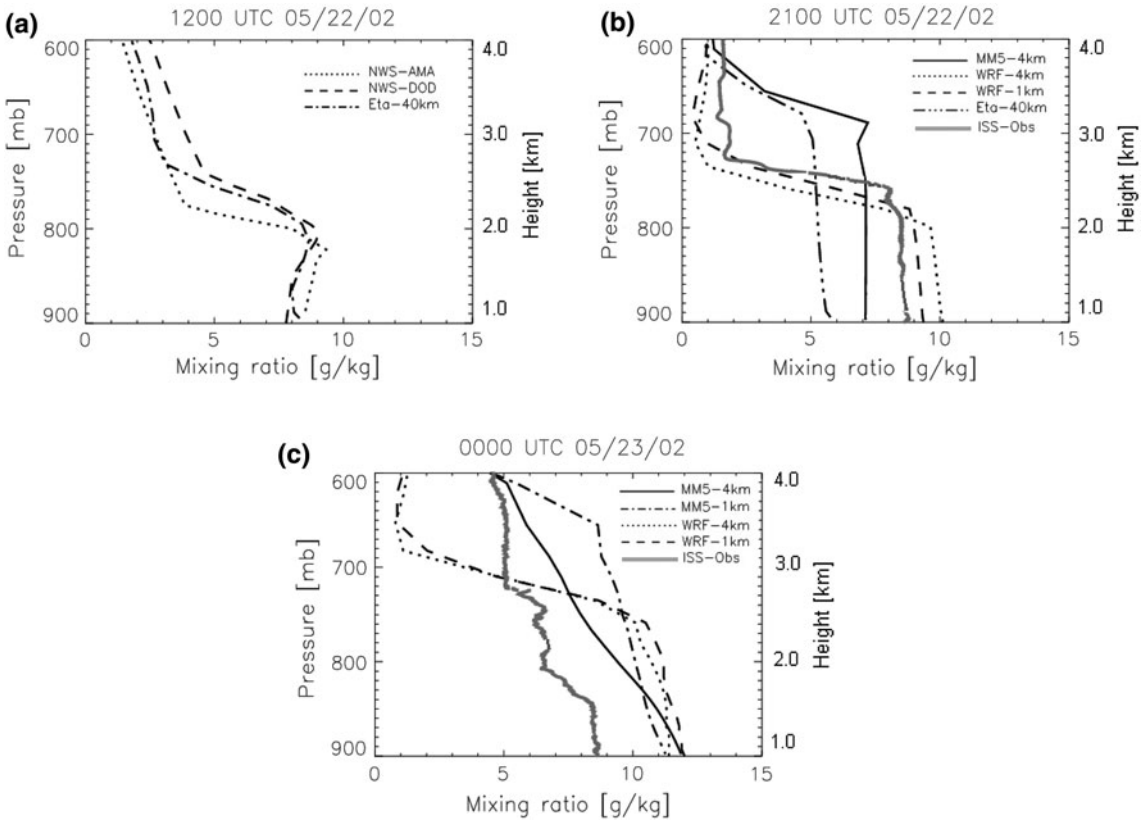

Fig. 8 Simulated and observed mixing ratio profiles: **a** 1200 UTC 22 May, before the dryline; **b** 2100 UTC 22 May; and **c** 0000 UTC 23 May 2002, when the dryline developed

2002), at 1-km resolution performed better in these limited simulations of boundary layer moisture compared to MM5 with Blackadar PBL scheme. At 0000 UTC 23 May, when the dryline was well developed, both WRF and MM5 models overestimated mixing ratios by $\sim$3.0 g kg^{-1} below 750 mb (Fig. 8c). During this time a strong moisture gradient prevailed over the IHOP domain, and the lower troposphere mixing ratio difference between DOD and AMA NWS stations was about 6.0 g kg^{-1} (data not shown). There was also a significant moisture difference between the Eta model output and the radiosonde observation at Homestead. A detailed discussion on moisture output from the numerical models during the 22 May 2002 dryline is presented in a Ph.D. dissertation (Weldegaber 2009).

Compared to the surface analysis of mixing ratio at 2100 UTC 22 May 2002 over the Oklahoma and Texas panhandles, as described in Wakimoto and Murphey (2009, see Fig. 1), mixing ratio profiles from the numerical models show discrepancies at Homestead. The discrepancy was exaggerated more at 0000 UTC 23 May 2002, where all numerical models show $\sim$2–3.0 g kg^{-1} excess boundary layer mixing ratio compared to the radiosonde profile at Homestead. This excessive simulated boundary layer moisture could be one among other possible reasons for the wrong model prediction of convection initiation during the 22 May 2002 dryline, which was not present in reality over the Homestead area.

5 Summary and conclusions

The 22 May 2002 null-convection dryline case is one of the most reported cases in the IHOP database. This dryline is generally stronger in terms of humidity contrast and confluence compared to other drylines. This study used high spatial and temporal resolution water vapor mixing ratio and boundary layer data from lidar (HARLIE, SRL), infrared interferometer (AERI), radiosondes and numerical weather prediction model (Eta, MM5, WRF) to test the hypothesis that sustained and deep moisture in the boundary layer is a precondition for a dryline convection initiation in the absence of strong synoptic forcing. The boundary layer moisture evolution during the 22 May dryline was also compared to other IHOP_2002 dryline cases.

The results indicate that the dryline on the late afternoon of 22 May was characterized by a lack of sustained and deep moisture compared to other dryline cases that triggered convective activity during IHOP_2002. Near-surface water vapor mixing ratios progressively increased through the day, but remained below 9.0 g kg^{-1}, while mixing ratios above 10.0 g kg^{-1} (>12.0 g kg^{-1} in case of 19 June) persisted in all the convective dryline cases. The relatively large surface mixing ratio values ($\geq$10.0 g kg^{-1}) on all the convective dryline cases and its sustained nature supports the hypothesis that sustained boundary layer moisture is important for convection initiation to occur during a dryline event. Although it lacked sustained and deep water vapor mixing ratio, the 22 May case has the highest lidar-measured boundary layer height and the most variable PBL height, an indication of active convection throughout the afternoon, compared to the other convective IHOP dryline cases. Thus, we can conclude that, no matter how active a case may be, lack of *abundant*, *deep*, and *sustained boundary layer moisture* inhibits storm initiation.

The CAPE values on 22 May were substantial, but so were the CIN values. As reported elsewhere (Demoz et al. 2006), there was substantial spatial variability in CAPE near the IHOP domain. The Rapid Update Cycle (RUC) simulated CAPE values at the Homestead site on 22 May were much exaggerated compared to the values computed from the radio sounding. To ascertain the effect of moisture in CAPE and thus convection, moisture values were increased by 20% resulting in a CAPE increase of 100%, while the CIN values decreased by 40%. A 40% increase in the boundary layer moisture values (i.e., approximately the amount that most of the convective dryline cases have in excess compared to the 22 May) double the sensitivity. This again supports the argument that sustained and deep moisture is a pre-requisite for convection initiation. In future work, the model response to variable moisture levels on the 22 May dryline will be investigated.

The simulated boundary layer mixing ratio profile from the WRF output agrees relatively well with the radio sounding observations when the dryline was established over the Homestead area around 2100 UTC. Increasing WRF horizontal grid resolution from 4 to 1-km has resulted to a slight improvement of model performance below 750 mb; however, there were no significant changes in the mixing ratio values in the upper levels. WRF performed better in simulating PBL moisture compared to the overestimated upper level (above 750 mb) moisture in MM5 at 2100 UTC. The moisture output from Eta, used as initial and boundary conditions in both MM5 and WRF simulations, compared well with the observations initially. However, the moisture output from Eta at other times (2100 UTC 22 May 2002) was $\sim$5.0 g kg^{-1} less compared to the radiosonde observations in the lower level, a substantial disagreement. All the numerical models show excess boundary layer moisture compared to the radiosonde observations over Homestead at 0000 UTC 23 May 2002. This excessive boundary layer moisture profile from the numerical models during the observed strong capping inversion was among the reasons for the wrong model prediction of deep convection initiation during the 22 May 2002 dryline, which was not present in reality over the Homestead area.

Acknowledgments This research was supported by National Science Foundation Grant ATM-0129605 and the National Aeronautical and Space Administration (NASA). The authors are indebted to the many colleagues and researchers that made IHOP_2002 and associated observations possible.

References

Arnott NR, Richardson Y, Wurman J, Rasmussen E (2006) Relationship between a weakening cold front, misocyclones, and cloud development on 10 June 2002 during IHOP. Mon Weather Rev 133:311–335

Atkins NT, Wakimoto RM, Ziegler CL (1998) Observations of the finescale structure of a dryline during VORTEX 95. Mon Weather Rev 126:525–550

Beebe RG (1958) An instability line development as observed by the tornado research airplane. J Meteor 15:278–282

Blackadar AK (1979) High resolution model of planetary boundary layer. Advances in environmental and scientific engineering, vol I. Gordon and Breach, New York, pp 50–85

Bluestein HB, Parker SS (1993) Modes of isolated, severe convective storm formulation along the dryline. Mon Weather Rev 121:1354–1372

Braun SA, Tao W (2000) Sensitivity of high-resolution simulations of Hurricane Bob (1991) to planetary boundary layer parameterizations. Mon Weather Rev 128:3941–3961

Buban MS, Ziegler CL, Rasmussen EN, Richardson YP (2007) The dryline on 22 May 2002 during IHOP: ground-radar and in situ data analyses of the dryline and boundary layer evolution. Mon Weather Rev 135:2473–2505

Cai H, Wen-Chau L, Weckwerth T, Flamant C, Murphey H (2006) Observations of the 11 June dryline during IHOP_2002—a null case for convection initiation. Mon Weather Rev 134:336–354

Chen F, Dudhia J (2001) Coupling an advanced land-surface/hydrology model with the Penn State/NCAR MM5 modeling system, part I: model description and implementation. Mon Weather Rev 129:569–585

Chen S-H, Sun W-Y (2002) A one-dimensional time dependent cloud model. J Meteor Soc Jpn 80:99–118

Crawford TM, Bluestein HB (1997) Characteristics of dryline passage during COPS-91. Mon Weather Rev 125:463–477

Crook A (1996) Sensitivity of moist convection forced by boundary layer process to low level thermodynamic fields. Mon Weather Rev 124:1767–1785

Demoz B, Flamant C, Weckwerth T, Whiteman D, Evans K, Fabry F, Girolamo P, Miller D, Geerts B, Brown W, Schwemmer G, Gentry B, Feltz W, Wang Z (2006) The dryline on 22 May 2002 during IHOP_2002: convective scale measurements at the profiling site. Mon Weather Rev 134:294–310

Feltz WF, Smith WL, Howell HB, Knuteson RO, Woolf H, Revercomb HE (2003) Near-continuous profiling of temperature, moisture, and atmospheric stability using the Atmospheric Emitted Radiance Interferometer (AERI). J Appl Meteor 42:584–597

Fujita T (1958) Structure and movement of a dry front. Bull Am Meteor Soc 39:574–582

Hane CE, Ziegler CL, Bluestein HB (1993) Investigation of the dryline and convective storms initiated along the dryline: field experiments COPS-91. Bull Am Meteor Soc 74:2133–2145

Janjic ZI (2002) Nonsingular implementation of the Mellor-Yamada Level 2.5 Scheme in the NCEP Meso Models. NCEP Office Note No. 437, 61 pp

Kock SE, Clark WL (1999) A nonclassical cold front observed during COPS-91: frontal structure and the process of severe storm initiation. J Atmos Sci 56:2862–2890

Lin Y-L, Farley RD, Orville HD (1983) Bulk parameterization of the snow field in a cloud model. J Climate Appl Meteor 22:1065–1092

Mailhot J, Chouinard C, Benoit R, Roch M, Verner G, Coté J, Pudykiewicz J (1989) Numerical forecasting of winter coastal storms during CASP: evaluation of the regional finite-element model. Atmos Ocean 27:24–58

Markowski P, Hannon C, Rasmussen E (2006) Observations of convection initiation "failure" from the 12 June 2002 IHOP deployment. Mon Weather Rev 134:375–405

Mellor GL, Yamada T (1982) Development of a turbulence closure model for geophysical fluid problems. Rev Geophys Space Phys 20:851–875

Miao Q, Geerts B (2007) Finescale vertical structure and dynamics of some dryline boundaries observed during IHOP. Mon Weather Rev 135:4161–4184

Miiller D, Wandinger U, Ansmann A (1999) Microphysical particle parameters from extinction and backscatter lidar data by inversion with regularization: theory. Appl Opt 38:2346–2357

Mills GA (1983) The sensitivity of a numerical prognosis to moisture detail in the initial state. Aust Meteor Mag 31:111–119

Parsons DB, Shapiro MA, Hardesty RM, Zamora RJ (1991) The finescale structure of a west Texas dryline. Mon Weather Rev 119:1242–1258

Perkey DJ (1976) A description and preliminary result from a finemesh model for qualitative precipitation. Mon Weather Rev 104:1513–1526

Richter H, Bosart LF (2002) The suppression of deep moist convection near the Southern Great Plains dryline. Mon Weather Rev 130:1665–1691

Schaefer JT (1973) A simulative model of dryline motion. J Atmos Sci 31:956–964

Schaefer JT (1986) The dryline. In: Ray PS (ed) Mesoscale meteorology and forecasting. American Meteorological Society, pp 549–572

Schwemmer GK (1998) Holographic Airborne Rotating Lidar Instrument Experiment. In: 19th International laser radar conference, NASA/CP-1998-207671/PT2, 623–626, Annapolis Maryland, 6–10 July 1998

Shaw BL, Pielke RA, Ziegler CL (1997) A three-dimensional numerical simulation of a Great Plains dryline. Mon Weather Rev 125:1489–1506

Skamarock WC, Klemp JB, Dudhia J (2001) Prototypes for the WRF (Weather Research and Forecasting) model. Preprints, Ninth conference on mesoscale processes, Fort Lauderdale, FL. American Meteorological Society, pp J11–J15

Staff Members (1963) Environmental and thunderstorm structures as shown by National Severe Storms Project observations in spring 1960 and 1961. Mon Weather Rev 91:271–292

Sun WY, Wu CC (1992) Formation and diurnal oscillation of dryline. J Atmos Sci 49:1606–1619

Trier SB, Chen F, Manning KW (2004) A study of convection initiation in a mesoscale model using high-resolution land surface initial conditions. Mon Weather Rev 132:2954–2976

Wakimoto RM, Murphey HV (2009) Analysis of a dryline during IHOP: implications of convection initiation. Mon Weather Rev 137:912–936

Wakimoto RM, Murphey HV, Browell EV, Ismail S (2006) The "Tripe Point" on 24 May 2002 during IHOP. Part I: airborne Doppler and LASE analyses of the frontal boundaries and convection initiation. Mon Wea Rev 134:231–134

Weckwerth TM, Parsons DB (2005) A review of convection initiation and motivation for IHOP_2002. Mon Weather Rev 134:5–22

Weckwerth TM, Wilson JW, Wakimato RM (1996) Thermodynamic variability within convective boundary layer due to horizontal convective rolls. Mon Weather Rev 124:769–784

Weckwerth TM, Parsons DB, Koch SE, More JA, LeMone MA, Demoz BB, Flamant C, Greets B, Wang J, Feltz WF (2004) An overview of the international H_2O project (IHOP_2002) and some preliminary highlights. Am Meteor Soc 85:253–277

Weiss CC, Bluestein HB (2002) Airborne pseudo-dual Doppler analysis of a dryline-outflow boundary intersection. Mon Weather Rev 130:1207–1226

Weiss CC, Bluestein HB, Pazmany AL (2006) Fine-scale radar observation of the 22 May 2002 dryline during the international H2O Project (IHOP_2002). Mon Weather Rev 134:273–293

Weldegaber MH (2009) Investigation of stable and unstable boundary layer phenomena using observations and a numerical weather prediction model; Ph.D. Dissertation. University of Maryland Baltimore County (UMBC), 2009

Wicker LJ, Skamarock WC (2002) Time-splitting methods using forward time scheme. Mon Weather Rev 130:2088–2097

Wilson JW, Roberts RD (2006) Summary of convective storms initiation and evolution during IHOP: observational and modeling perspective. Mon Weather Rev 134:23–47

Wilson JW, Schreiber WE (1986) Initiation of convective storms at radar-observed boundary-layer convergence lines. Mon Weather Rev 114:2516–2536

Wisse JSP, De Arellano JV (2004) Analysis of the role of the planetary boundary layer schemes during a severe convective storm. Ann Geophys 22:1861–1874

Xue M, Martin WJ (2006) A high-resolution modeling study of the 24 May 2002 dryline case during IHOP. Part I: numerical simulation and general evolution of the dryline and convection. Mon Weather Rev 134:149–171

Ziegler CL, Rasmussen EN (1998) The initiation of moist convection at the dryline: forecasting issues from a case study perspective. Weather Forecast 13:1106–1131

Ziegler CL, Lee TJ, Pielke RA (1997) Convection initiation at the dryline: a modeling study. Mon Weather Rev 125:1001–1026